*Bangladesh Journal of Physics, Vol. **30**, Issue 1, pp. 1–11, June 2023*

Invited Review Article

A BRIEF OVERVIEW TO THE ELECTRONIC BAND STRUCTURES OF NICKELATES AND CUPRATES IN THE GROUND STATE

MD. ENAMUL HAQUE, AYESHA SIDDIKA BORNA, S. H. NAQIB*

Department of Physics, University of Rajshahi, Rajshahi 6205, Bangladesh

**Corresponding author e-mail: salehnaqib@yahoo.com*

Received on 14.06.2023, Accepted for publication on 17.06.2023

DOI: *https://doi.org/10.3329/bjphy.v30i1.68372*

ABSTRACT

The discovery of infinite-layer nickelates opens up a new era of high-T_c superconductors. The nickelate compounds are almost isostructural to the high-T_c cuprates. Both cuprates and nickelates are insulators in the absence of self-doping and become superconducting upon doping the CuO_2 and NiO_2 planes, respectively. The mechanism of high-T_c superconductivity in correlated electronic systems will undoubtedly gain new insights from a verification of the similarities and differences between these oxides. In this brief report, we study the published electronic band structures of nickelates and cuprates in the undoped ground state. By comparing and contrasting the ground state electronic band structures of cuprates and nickelates, we have made an attempt to understand the common electronic features which can be important for the emergence of superconductivity upon carrier doping.

Keywords: Nickelate superconductors; High-T_c cuprates; Electronic band structure; Strongly correlated electronic systems

1. INTRODUCTION

A long-standing issue in the phenomenology of strongly correlated transition-metal oxides (TMO) is the nature of the insulator-metal transition and its close connection to the character of the electronic band structure including the band gap. The insulating phase of the parent compound falls mainly into two categories: Mott-type or the charge-transfer-type. In the Mott insulators, band gap is formed by the upper and lower Hubbard bands where the on-site Coulomb potential U is less than the charge-transfer energy characterized by the ligand oxygen 2p levels. On the other hand, the gap in the energy spectrum in a charge-transfer insulator is formed by the oxygen 2p states and the upper Hubbard band. Physically, these two scenarios give rise to very different pictures upon carrier doping. In one, the carrier sits on the transition-metal atom and in the other, it sites on the oxygen sites. The classification of the energy gap alone, however, does not control the overall nature of the doped electronic states. For example, the undoped cuprate La_2CuO_4 (LCO) and undoped La_2NiO_4 (LNO) are isostructural and both share CuO_2/NiO_2 plane where the doped charge carriers reside and take part in Cooper pairing. LCO is a prototypical high-temperature superconductor with active itinerant carriers setting at around 0.05 holes in the CuO_2 plane [1]. In contrast, LNO becomes metallic for a hole content ~0.08 [2].

Recently, it was reported that the doped infinite-layer nickelate $Nd_{0.8}Sr_{0.2}NiO_2$ exhibited superconductivity [3]. In that the nickel $3d_{x^2-y^2}$ orbital forms a highly correlated system on the two-dimensional square lattice near the half-filling, the infinite layer nickelate $RNiO_2$ (R: a rare earth

element) resembles the cuprates. However, the presence of self-doping marks a significant distinction from the cuprates; additional Fermi pockets are formed by rare earth-layer orbitals. In this sense, the parent compounds of the infinite-layer nickelates could be seen as a system that, due to the self-doping, is not a Mott insulator. The superconductivity in nickelate is most likely unconventional, and the correlation effect is expected to play an important role. The existence of the itinerant rare earth-layer orbitals would result in Kondo-like physics [3]. The physics of the Zhang-Rice singlet may emerge if the holes are doped into the oxygen 2p orbitals [3].

The emergence of superconductivity in the doped infinite layer nickelates $RNiO_2$ (R = La, Pr, Nd) is of great interest mainly because the undoped nickelates share a number of common features with the undoped cuprates [4]. Hence by verifying the commonalities and differences between these oxides will certainly give new insights into the mechanism of high-T_c superconductivity in correlated electron systems. In this work, we wish to compare and contrast the electronic band structures of nickelates and cuprates in the ground state.

The rest of the article is constructed as follows. Section 2 describes very briefly the structural features and electronic phase diagrams of cuprates and nickelates. In the Section 3 we have looked at the electronic band structures of these strongly correlated electronic systems in the ground state. Conclusions of this work can be found in Section 4.

2. STRUCTURES AND ELECTRONIC PHASE DIAGRAMS OF CUPRATES AND NICKELATES

Cuprate superconductors are complex tetragonal or almost tetragonal materials. They do not have the simple perovskite type structure. However, several important features of the ideal perovskite structure are present in the cuprates. The ideal perovskite structure is cubic (Fig. 1). The general formula of a perovskite compound is ABX_3.

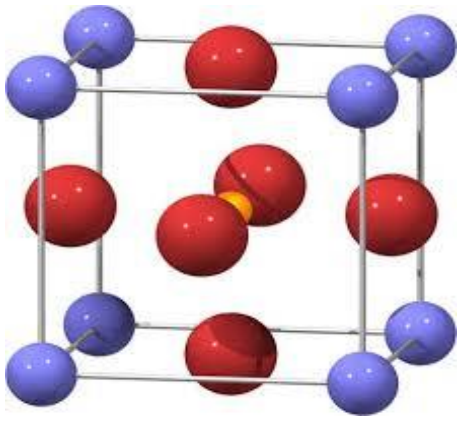

Fig. 1 Cubic perovskite unit cell. Blue spheres represent the A cation, yellow spheres represent B cation, and red sphere represent oxygen anions forming an octahedron.

The anion X (typically oxygen) and the cation A (typically Sr or Ba for cuprates) are relatively large, determining the size of the structure. The smaller B cation (Cu for cuprates) occupies the interstices of the A-X network. The six anions surrounding the B cation form an octahedron.

The layered structure makes the high-T_c cuprates very anisotropic. All the cuprates contain CuO_2 planes, with a simple square (or slightly orthorhombic) lattice. Cuprates can have one or more CuO_2 planes per formula unit. The CuO_2 planes are often adjacent to purely ionic interleaving AX planes and the O atoms coordinate the Cu atoms of the CuO_2 plane similar to the ordinary perovskite structure. Also, the picture of the perovskite rectangular framework of anions and cations holds true for the cuprate structure as well. Hence, the cuprates are termed as modified perovskite type compound. In some cuprates, the copper-oxide layers are isolated as in the perovskite, but in others two or three copper-oxide layers are stacked directly above each other, as shown in Fig. 2.

Hole-doped cuprate superconductors have played an indispensable role in the exciting development of high temperature superconductivity (HTS) science and technology over the last 37 years. More than 200 cuprate superconductors have been found. The observation began with finding the superconductivity up to 35 K in the Ba-doped La_2CuO_4 ternary compound by J. G. Bednornz and K. A. Muller [5], followed immediately by the discovery of superconductivity at 93 K in the new oxygen-doped $YBa_2Cu_3O_7$ quaternary compound by C. W. Chu and M. K. Wu and their team in 1987 [6].

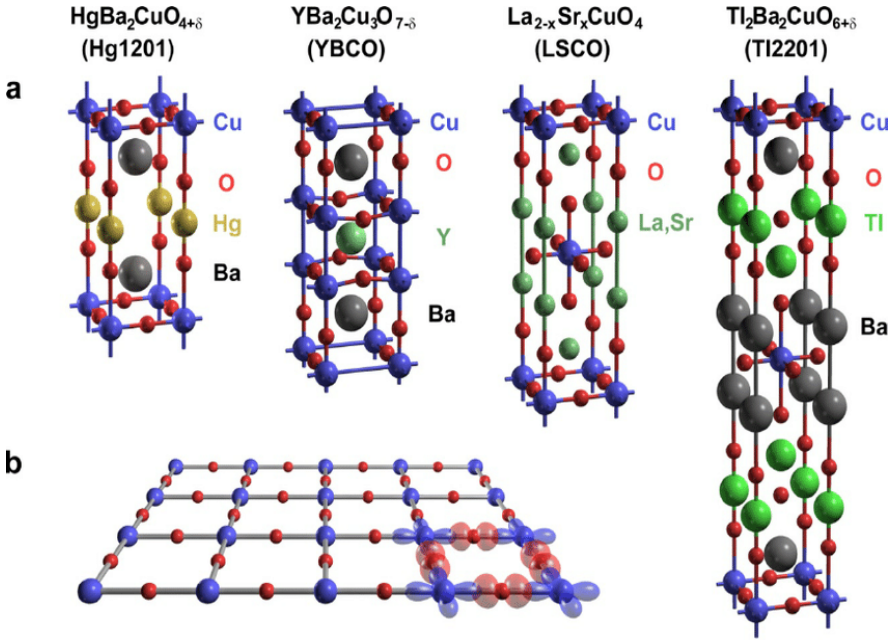

Fig. 2 (a) Crystal structures of several hole doped cuprates and (b) the view of the CuO_2 plane.

Doping results in adding charge carriers into the parent compounds. This is achieved either by cationic substitution and/or by oxidation. All cuprates are very sensitive to carrier doping and are superconducting for a particular range of doping level. The states of the CuO_2 layers depend on how the compound is doped. LSCO ($La_{2-x}Sr_xCuO4$) is doped by cationic substitution. In this case, Sr^{2+} ion is substituted for a La^{3+} ion and there would be (1+x) holes per unit cell spread over the CuO_2

plane [7]. For YBCO ($Y_{1-x}Ca_xBa_2Cu_3O_{7-\delta}$), hole doping is done by oxidation or cationic substitution [8]. For cationic substitution, Ca^{2+} ion is often substituted for Y^{3+} ion, for example [9].

In high-T_c cuprates, the electronic states are very sensitive to carrier doping and are also dependent on the temperature. The generic behavior of cuprates according to the electronic phase diagram (T-p), shown in Fig. 3, is described below.

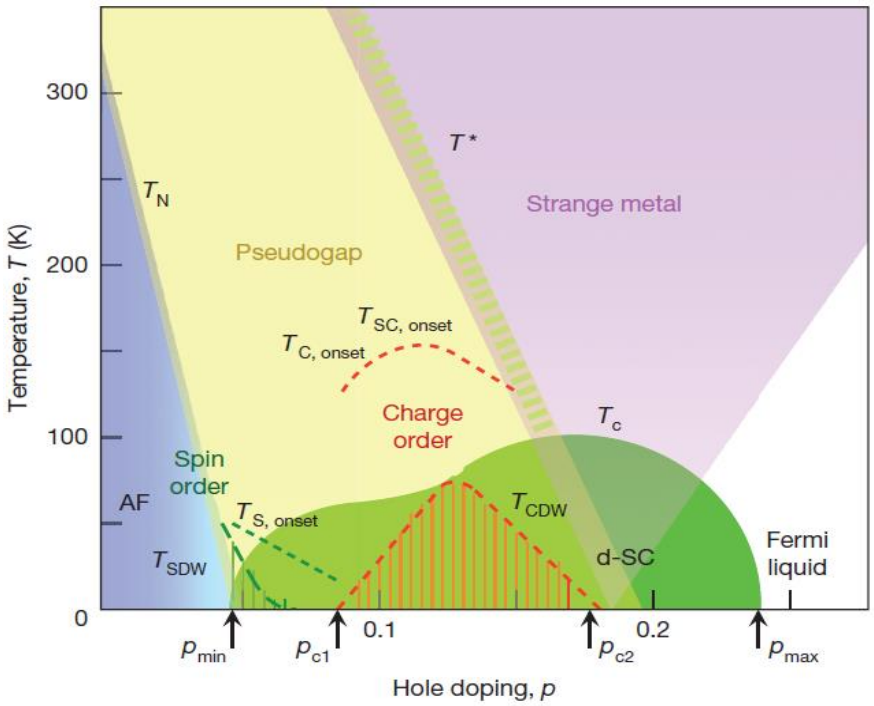

Fig. 3 The generic electronic phase diagram of hole doped cuprates as a function of temperature and doping [10]. Various electronic ground states are shown. Further details can be found in Ref. [10].

Antiferromagnetic region: At zero doping (p = 0), the parent compound is a Mott-Hubbard insulator and up to a few hundred Kelvin, the system shows an antiferromagnetic behaviour. As the system is doped, the antiferromagnetic order is markedly disrupted with the Neel temperature T_N falling rapidly to zero.

Spin glass region: Some cuprates have a spin glass phase between the antiferromagnetic and superconducting regions. It is a disordered magnetic phase with no long-range magnetic ordering. Below the spin glass transition temperature T_g, a highly irreversible metastable state is found with random freezing of spins.

Superconducting region: The onset of superconductivity is around p ~ 0.05. With increasing doping level (p), T_c rises, attains maximum value and then falls back to zero with further increase in the hole content. Superconductivity exists in the region $0.05 < p < 0.27$. T_c varies approximately parabolically with hole content p which can be expressed by an empirical relation given by [11]:

$$T_c(p) = T_c^{max}[1-82.6\,(p-0.16)]^2$$

where, T_c^{max} = maximum T_c at the optimum doping (p ~ 0.16).

Fermi-liquid region: The region of the phase diagram with higher doping levels of cuprates is the Fermi-liquid region. In a Landau Fermi-liquid, the free electron mass (m_e) is changed to m^* through electron-electron interaction. The particles are called quasi-particles. The quantum numbers describing the quantum states of the electrons are still valid. The dynamic properties will change. Quasi-particle scattering rate at low-T is expected to be proportional to T^2. For Fermi-liquids, the resistivity $\rho \sim T^2$, at low temperature. There is a well-defined Fermi surface at low-T for a Fermi-liquid. Fermi-liquid picture can explain part of the phase diagram in the overdoped region.

Non-Fermi-liquid region: The region of the phase diagram between the pseudogap region and the Fermi liquid region is called the non-Fermi-liquid region. This is above the superconducting dome. The thermodynamic properties in this region are not very different from that in the Fermi-liquid region. But the transport properties deviate from that in the Fermi-liquid region.

Pseudogap region: One of the most challenging sections of the phase diagram of the high-T_c cuprates is the pseudogap region [12-14]. There is a suppression of the density of states around the Fermi energy in the normal state of the underdoped cuprates. This is called the pseudogap or the normal state gap. The effect of pseudogap is observed experimentally below a certain temperature, frequently denoted by T^*.

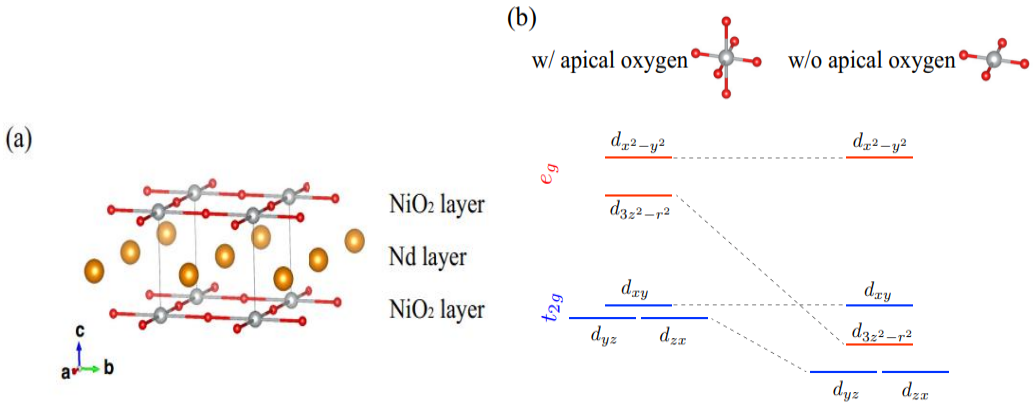

Fig. 4. (a) The crystal structure of $NdNiO_2$ and (b) the corresponding square-planar crystal field (right) [3].

The crystal structure and local electronic configuration of an infinite-layer nickelate $RNiO_2$ (R = La, Pr, Nd) are shown in Figs. 4. Like cuprates, it has a layered structure, with alternating NiO_2 and R layers. In the infinite-layer structure, the apical oxygens are absent. In this particular structure, it is estimated that the neodymium is a 3^+ cation and oxygen is a 2^- anion, giving the nickel a 1^+ valence.

The square planner crystal field is shown in Fig. 4(b). The electronic structure is stabilized by the $d_{3z^2-r^2}$ orbital; its onsite level becomes comparable to those of the d_{xy}, d_{yz}, and d_{zx} orbitals (called t_{2g} orbitals in an octahedral environment). Therefore, the $d_{x^2-y^2}$ orbital is isolated from the other 3d orbitals in the energy diagram [3].

Figs. 5 show the electronic phase diagram of $Nd_{1-x}Sr_xNiO_2$ thin films grown on the $SrTiO_3$ substrate, including their temperature dependent in-plane resistivities. The resistivity of the parent material does not show a strong insulating behavior but rather discloses a weakly insulating behaviour at low temperatures [3].

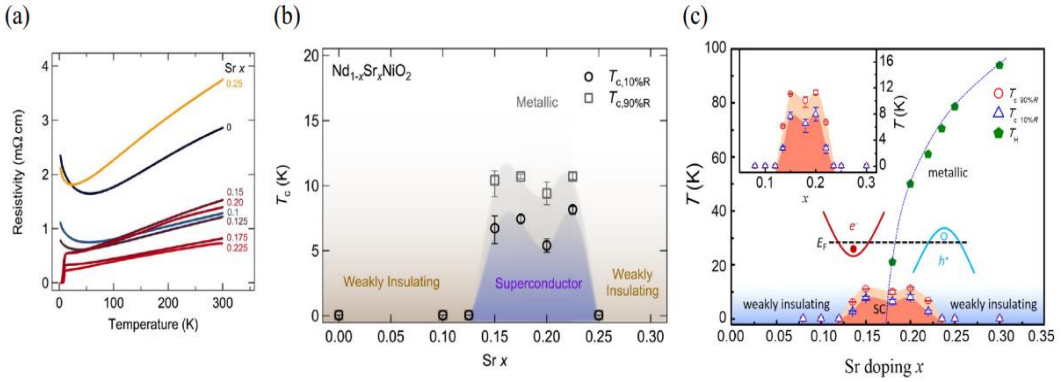

Fig. 5 (a) Doping (x) dependence of the resistivity and (b,c) temperature-doping phase diagram of $Nd_{1-x}Sr_xNiO_2$ thin film samples grown on $SrTiO_3$ substrate. Further details can be found in Ref. [3].

The undoped nickelates often show self-doping effects and becomes metallic. We will treat such systems as *undoped* since no external doping elements are introduced.

The term 'weakly insulating' refers to the slight increase in resistance that occurs at low temperatures. Superconductivity is observed in the region where the strontium doping concentration is $0.125 \leq x \leq 0.25$, and in this region a dome-shaped T_c is observed. The superconductivity disappears in the over doped region and the resistivity increases at low temperature [3]. The doping dependent variations in the superconducting transition temperature are qualitatively similar to that of high-T_c cuprates. According to the current theory [3], this nickel-based system represents a brand-new class of superconducting materials because their phase diagram suggests that they are correlated metals with distinct multiband features. Using a variety of experimental and theoretical tools, these systems have been quickly examined from numerous angles. It has been established that the rare-earth infinite-layer nickelates support a distinctive multiband interplay, on top of which electronic correlations develop and define the fundamental characteristics of these systems. The rare earth states add additional distinctive components, such as the self-doping effect [4]. There is now experimental proof of developing antiferromagnetic order, which has been theorized to be responsible for the emergence of superconductivity in these materials [15].

3. ELECTRONIC BAND STRUCTURES OF CUPRATES AND NICKELATES IN THE UNDOPED STATE

The range of energy levels that electrons may have within a solid, as well as the ranges of energy that they may not have (called band gap or forbidden bands), are described by the electronic band structure (or simply the band structure). By analyzing the allowed quantum mechanical wave functions for an electron in a large, periodic lattice of atoms or molecules, band theory derives these bands and band gaps. Many physical properties of solids, such as the charge transport and optical parameters forming the foundation of the understanding of all solid-state devices, have been explained by the electronic band structure. We have shown the band structures of several cuprates and nickelates in this section.

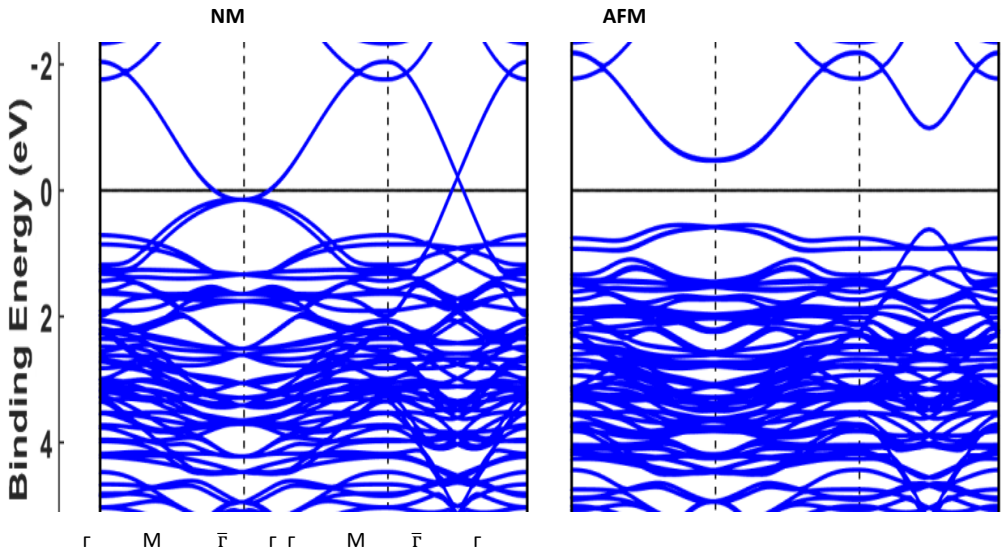

Fig. 6 Theoretical electronic band dispersions of La_2CuO_4 for the nonmagnetic (NM) and antiferromagnetic (AFM) phases [16].

La_2CuO_4: The band structure of single CuO_2 layer La_2CuO_4 in the nonmagnetic (NM) and antiferromagnetic (AFM) phase are shown in Fig. 6. Here and throughout, we will distinguish the in-plane oxygen atoms from the apical oxygen atoms as O and O_z, respectively.

Experimentally, it was found that in the ground state La_2CuO_4 is an AFM insulator. Thus, we focus our attention to this particular electronic state.

Figure 6 shows that the AFM state of La_2CuO_4 is stabilized with a band gap of approximately 1.0 eV. This gap develops in the half-filled Cu $d_{x^2-y^2}$ dominated band by splitting the up and down spin anti-bonding bands. A consequence of this splitting is the generation of a flat (almost non-dispersing) electronic band below the Fermi level (placed at zero energy). Additionally, distinct splitting is produced in the bonding and anti-bonding bands of Cu d_{z^2}/O_z p_z. In the AFM phase, the conduction states are dominated by the $d_{x^2-y^2}$ orbitals of Cu. However, the valence states are not dominated by the Cu $d_{x^2-y^2}$ orbital but consist of almost equal contributions (around -0.55 eV) from the $d_{x^2-y^2}$/O $p_x + p_y$ and d_{z^2}/O_z p_z orbitals [16]. For completeness, we have also shown that band structure in the nonmagnetic phase. This phase is metallic and is not found in nature. Undoped La_2CuO_4 is an AFM insulator.

$YBa_2Cu_3O_6$: $YBa_2Cu_3O_6$ is a tetragonal system with two CuO_2 layers in the formula unit. This undoped compound is also an AFM insulator in the ground state. In this parent compound, the oxygen deficiency in the $CuO_{1-\delta}$ chain sites running along the crystallographic b-direction is maximum ($\delta = 1$). Oxygenation of the chain adds holes in the CuO_2 layers and superconductivity emerges when $\delta \sim 0.6$ [17-19]. The electronic band structure of $YBa_2Cu_3O_6$ is shown below in Fig. 7.

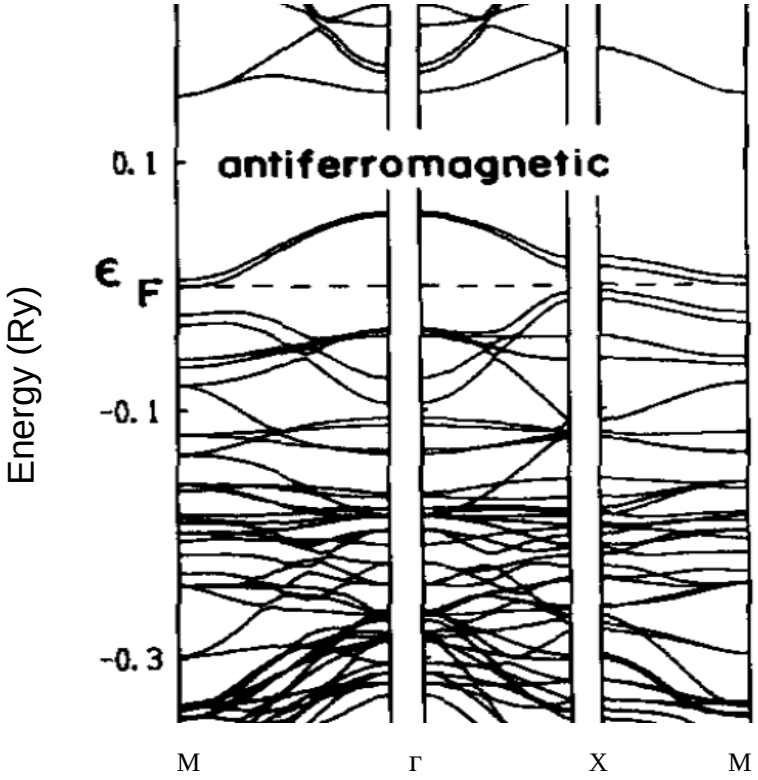

Fig. 7 The calculated electronic band structure for AFM $YBa_2Cu_3O_6$ [20].

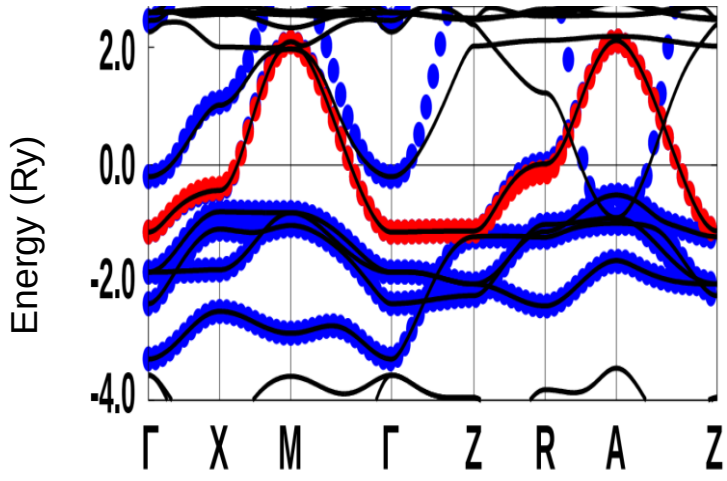

Fig. 8 Electronic band structure of $LaNiO_2$ crystal in the (AFM) phase [21]. The Fermi level is placed at 0 eV.

In the AFM phase, the valence band of $YBa_2Cu_3O_6$ below the Fermi level is due to the hybridized Cu 3d and O 2p electronic orbitals [20]. The AFM and insulating electronic band structure are also characterized by flat bands below the Fermi level. The degree of electronic dispersion of these bands is relatively higher in $YBa_2Cu_3O_6$ compared to that in La_2CuO_4.

$LaNiO_2$: The electronic band structure of $LaNiO_2$ is shown below (Fig. 8). This compound is AFM with metallic character. The metallicity arises due to self-doping. This self-doping gives rise to hole-like Fermi surface. The band structure has been calculated using the Density functional theory (DFT) methodology [21].

In this compound, besides the Ni $d_{x^2-y^2}$ orbital, additional bands around the Fermi level are of predominant La 5d character which overlaps with the former. It is worth noticing that the La-5d bands extend below the Fermi level (E_F) despite their centre of gravity being considerably above E_F. In band structure of $LaNiO_2$, single-band (Ni $d_{x^2-y^2}$, red dots) and other 5-bands (La 5d and Ni 3d, blue dots) are superimposed on the DFT band structure (black lines) [21]. Both the band structure of cuprates (La_2CuO_4) and nickelate ($LaNiO_2$) are characterized by flat bands below the Fermi Level.

$NdNiO_2$: The electronic band structure of $NdNiO_2$ is presented below (Fig. 9). This compound is also AFM with metallic character. The metallicity originates from self-doping just as in $LaNiO_2$. This self-doping gives rise to hole-like Fermi surface. The band structure has been calculated using the Density functional theory (DFT) methodology [21].

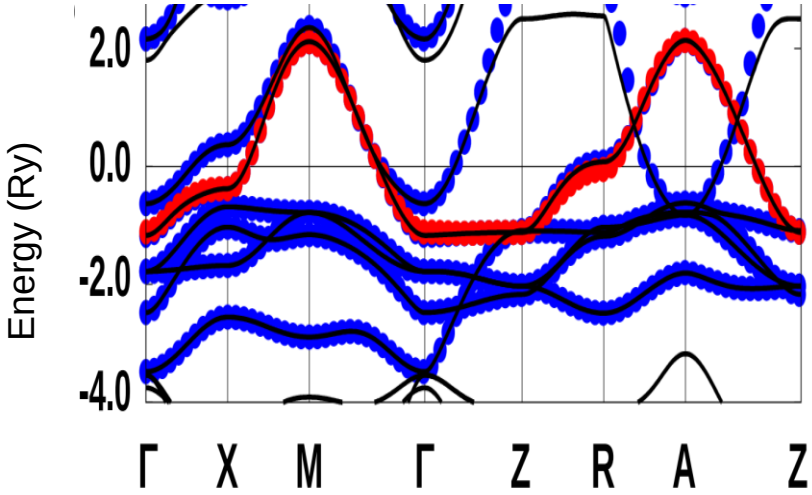

Fig. 9 Electronic band structure of $NdNiO_2$ crystal in the (AFM) phase [21]. The Fermi level is placed at 0 eV.

In this compound, besides the Ni $d_{x^2-y^2}$ electronic orbital, additional bands around the Fermi level are of predominant Nd 5d character which overlaps with the former. In the band structure of $NdNiO_2$, single-band (Ni $d_{x^2-y^2}$, red dots) and other 5-bands (Nd 5d and Ni 3d, blue dots) are superimposed on the DFT band structure (black lines) [21]. The band structure of $NdNiO_2$ is very similar to that of $LaNiO_2$ both qualitatively and quantitatively.

4. DISCUSSION AND CONCLUSIONS

From the study of the electronic band structures of cuprates and nickelate, we find that all of these systems consist of a flat (non-dispersing) band below the Fermi level. This indicates a type of band structures with constant electronic energy, independent of the crystal momentum. The key feature of the flat band is that the charge carriers in it have very small group velocity and very high charge carrier effective mass. The electronic energy density of states is also highly enhanced in the non-dispersive energy bands. All these features are sign of strong electronic correlation in a material.

Both the cuprate and nickelate superconductors are strongly correlated electronic systems. To understand these systems, one must consider the electron-electron interactions. These flat bands are essential ingredients for the dominant physics in cuprates and nickelates, potentially leading to all kinds of interesting physics like magnetic order, superconductivity, etc.

For $LaNiO_2$, the flat bands are seen around -0.67 eV, -1.17 eV, -1.08 eV, -0.75 eV along X-M, Γ-Z, Z-R, R-A-Z, directions in the first Brillouin zone (BZ), respectively, in the electronic band structure. For $NdNiO_2$, the flat bands are seen around -0.80 eV, -1.16 eV, -1.20 eV, -0.98 eV along X-M, Γ-Z, Z-R, R-A-Z, directions in the first BZ, respectively, in the electronic band structure. For La_2CuO_4, the flat bands are seen around -0.60 eV, -0.78 eV, -0,96 eV, -0.96 eV along Γ-M-$\bar{\Gamma}$, Γ-M, M-$\bar{\Gamma}$, $\bar{\Gamma}$-Γ, directions in the first BZ, respectively, in the electronic band structure. For $YBa_2Cu_3O_6$, the flat bands are seen around -0.29 eV, -0.50 eV, -0.57 eV along M-Γ, Γ-X, M-Γ-X, directions in the first BZ, respectively, in the electronic band structure. In all the systems, the flat bands are close to and below the Fermi level.

The following table shows, at a glance, the energy positions (with respect to Fermi level) of the flat bands and their relevant directions within the BZ.

Table 1: Energy positions (with respect to the Fermi level) of the flat bands and their relevant directions within the BZ.

Compound	Position (eV)	Direction	Ground state	Structure
$NdNiO_2$	-0.80	X-M	AFM/Self-doped	Tetragonal
	-1.16	Γ-Z		
	-1.20	Z-R		
	-0.98	R-A-Z		
$LaNiO_2$	-0.67	X-M	AFM/Self-doped	Tetragonal
	-1.17	Γ-Z		
	-1.08	Z-R		
	-0.75	R-A-Z		
La_2CuO_4	-0.60	Γ-M-$\bar{\Gamma}$	AFM/Insulator	Tetragonal
	-0.78	Γ-M		
	-0.96	M-$\bar{\Gamma}$		
	-0.96	$\bar{\Gamma}$-Γ		
$YBa_2Cu_3O_6$	-0.29	M-Γ	AFM/Insulator	Tetragonal
	-0.50	Γ-X		
	-0.57	M-Γ-X		

A common feature of copper-oxide compounds is the presence of strong antiferromagnetic Cu spin correlations in the CuO_2 planes. The in-plane copper ions in the undoped compounds are in the state of Cu^{2+} ($3d^9$) and have one hole with a spin S = 1/2 in the third shell. A strong super exchange interaction (via the oxygen ions) between the Cu spins gives rise to a three-dimensional long-range AFM order in La_2CuO_4 and $YBa_2Cu_3O_6$ compounds [22].

In our study, the important findings were that, in the AFM phase, the band form close to the Fermi level is dominated by the Cu $3d_{x^2}$-d_{y^2} orbitals in both cuprates and nickelates. But in the case of nickelates, another band contributes: the La/Nd 5d orbitals. Flat bands close to the Fermi level are another defining feature of both cuprates and nickelates in the undoped parent ground state. These flat bands are responsible for the strong electronic correlations in these systems.

REFERENCES

[1] S. H. Naqib, J. R. Cooper, J. L. Tallon, and C. Panagopoulas, Physica C **387**, 365 (2003).

[2] H. Eisaki, S. Uchida, T. Mizokawa, H. Namatame, A. Fu-jimori, J. Van Elp, P. Kuiper, G. Sawatzky, S. Hosoya, and H. Katayama-Yoshida, Physical Review B **45**, 12513 (1992).

[3] Y. Nomura and R. Arita, Reports on Progress in Physics **85**, 5 (2022).

[4] A. S. Botana, F. Bernardini, and A. Cano, Journal of Experimental and Theoretical Physics **132**, 618 (2021).

[5] J. G. Bednorz and K. A. Müller, Z. Phys. B **64**, 189 (1986).

[6] M. K. Wu, J. R. Ashurn, C. J. Torng, P. H. Hor, R. L. Meng, L. Gao, Z. J. Huang, Y. Q. Wang, and C. W. Chu, Phys. Rev. Lett. **58**, 908 (1987).

[7] R. S. Islam, J. R. Cooper, J. W. Loram, and S. H. Naqib, Phys. Rev. B **81**, 054511 (2010).

[8] S. H. Naqib and Anita Semwal, Physica C 425, **14** (2005).

[9] S. H. Naqib and R. S. Islam, Journal of Superconductivity and Novel Magnetism **27**, 337 (2014).

[10] B. Keimer, S. A. Kiveson, M.R. Norman, S. Uchida, and J. Zaanen, Nature **518**, 179 (2015).

[11] M. R. Presland, J. L. Tallon, R. G. Buckley, R. S. Liu, and N. E. Flower, Physica C **176**, 95 (1991).

[12] S.H. Naqib and R.S. Islam, Sci. Rep. **9**,14856 (2019).

[13] T. Timsuk and B. Satt, Rep. Prog. Phys. **62**, 61 (1999).

[14] S. H. Naqib and R. S. Islam, Supercond. Sci. Technol. **21**, 105017 (2008).

[15] L. E. Chow and A. Ariando, Frontiers in Physics **10**, 20 (2022).

[16] C. Lane *et al*., Phys. Rev. B **98**, 125140 (2018).

[17] S. H. Naqib, J. R. Cooper, J. L. Tallon, R. S. Islam, and R. A. Chakalov, Phys. Rev. B **71**, 054502 (2005).

[18] S. H. Naqib, J. R. Cooper, R. S. Islam, and J. L. Tallon, Phys. Rev. B **71**, 184510 (2005).

[19] S. H. Naqib, J. R. Cooper, and J. W. Loram, Phys. Rev. B **79**, 104519 (2009).

[20] B. Szpunar, V. H. Smith Jr, and R. W. Smith, Physica C **152**, 91 (1988).

[21] M. Kitatani, L. Si, O. Janson, R. Arita, Z. Zhong, and K. Held, npj Quantum Materials **5**, 59 (2020).

[22] N. Plakida, in *High-Temperature Cuprate Superconductors: Experiment, Theory, and Applications*, Springer Series in Solid-State Sciences (SSSOL, volume 166) (2010).